Acquisition of GNSS Signals in Urban Interference Environment

MATTHIAS WILDEMEERSCH, Member, IEEE
Singapore University of Technology and Design

CORNELIS H. SLUMP, Member, IEEE
University of Twente
The Netherlands

ALBERTO RABBACHIN, Member, IEEE
Massachusetts Institute of Technology

In urban environment Global Navigation Satellite System (GNSS) signals are impaired by strong fading and by the presence of several potential sources of interference that can severely affect the acquisition. The work presented here evaluates the acquisition performance for the most common acquisition strategies in terms of receiver operating characteristics (ROC) and studies the impact of fading and interference on the acquisition performance. Two different interference scenarios are considered: a single interferer and a network of interferers. We present a framework to evaluate the GNSS acquisition performance with respect to all relevant system parameters that jointly considers the acquisition method, the effect of radio signal propagation conditions, and the spatial distribution of the interfering nodes.

Manuscript received February 16, 2012; revised November 6, 2012, March 12, 2013, March 19, 2013; released for publication May 15, 2013.

DOI. No. 10.1109/TAES.2013.120094

Refereeing of this contribution was handled by A. Dempster.

This work has partly been fulfilled at the Joint Research Centre of the European Commission, and has been supported by the A* STAR Research Attachment Programme and the European Commission Marie Curie International Outgoing Fellowship under Grant 2010-272923.

Authors' addresses: M. Wildemeersch, Institute for Infocomm Research, A*STAR, 1 Fusionopolis Way, 21-01 Connexis South Tower, Singapore 138632. E-mail: (matthias.wildemeersch@gmail.com). C. H. Slump, Signals and Systems Group, University of Twente, Drienerlolaan 5, 7500 AE Enschede, the Netherlands; A. Rabbachin, Laboratory for Information and Decision Systems (LIDS), Massachusetts Institute of Technology, 77 Massachusetts Avenue, Cambridge, MA 02139.

I. INTRODUCTION

Spread spectrum (SS) techniques have been first applied in the military domain because of their intrinsic characteristics, such as the possibility to hide the signal under the noise floor, the low probability of interception and its robustness against narrowband interference [1]. Other beneficial properties have lead to the widespread use of direct sequence spread spectrum (DSSS) in commercial applications. In particular, thanks to the large transmission bandwidth that allows precise ranging, DSSS has been applied for location and timing applications such as Global Navigation Satellite Systems (GNSS).

For a correct signal reception, the alignment between the transmitted spreading code and the locally generated sequence is fundamental. Code synchronization in DSSS systems consists typically of two sequential parts: acquisition and tracking. The acquisition yields a coarse alignment and the subsequent tracking ensures a continuous fine alignment of the phases. The code acquisition is a binary detection problem, where the decision has to be made for each possible code phase and Doppler frequency. These two variables constitute a two-dimensional search space which is discretized into different cells. Every detection or estimation process is composed of an observation block and a decision or estimation block [2], In the observation block the cells in the search space are computed by downconverting the incoming signal, followed by a correlation with the local replica of the SS sequence. The cell values depend on the implementation details for the computation of a single cell (e.g. integration time), the presence of the signal of interest (SoI), noise and interference, and the channel conditions. The cell values are hence random variables (RVs) with their statistical distribution [3], which we call the cell statistics. In the decision block a decision variable is calculated based on single or multiple cells of the search space, which determines the presence or absence of the SoI. Different acquisition strategies received wide research interest in the past [4–8]. The most popular acquisition strategy consists in comparing the maximum value of the search space with a threshold value and is called the threshold crossing (MAX/TC) criterion [5]. Another common acquisition strategy for GNSS signals relates the maximum cell in the search space to the second maximum, which has as main advantage to maintain the probability of false alarm independent of the noise power density [9].

The acquisition performance is well described in the presence of additive white Gaussian noise (AWGN). Recent studies show that, in urban environment, the detection of the GNSS signal can be seriously challenged by sources of unwanted interference [10–14], in addition to the channel fading inherent to environments with a large amount of obstacles. For DSSS systems the impact of channel fading on the acquisition performance has been studied in [15–22]. However, the analysis is focused on the acquisition by mobile terminals in cellular networks. The acquisition of GNSS signals differentiates itself from

the acquisition in direct sequence-code division multiple access (DS-CDMA) networks by the extremely low GNSS signal power and by the different fading distributions that affect the SoI and the interference. Hence, considering that GNSS is a critical infrastructure, it is relevant to study the impact of different sources of interference to assess its performance in urban environment [23]. For single interferers the impact of narrowband interference has been studied in [10]. Further, [13] and [14] discuss the interference originating from digital video broadcasting - terrestrial (DVB-T) transmissions. None of the transmission bands for DVB-T are active within the frequency bands allocated for GNSS signals. However, some of the harmonics of DVB-T signals transmitted in the UHF IV and UHF V bands coincide with the GPS L1 or Galileo E1 bands and therefore these signals can be potential sources of unintentional interference. Due to the increasing number of mobile devices equipped with radio transmitters, we can expect a drastic proliferation of possible sources of interference [24]. Although legal policies are established to protect the GNSS bands, there exist future realistic scenarios such as multi-constellation GNSS [25], the deployment of pseudolites [26–28] and ultra wideband (UWB) transmitters [29, 30], where the interference can originate from multiple transmitters [31], and where literature specifically warns of the severe interference effects and the resulting performance degradation inflicted on GNSS receivers. Another possible threat for GNSS systems are cognitive radio (CR) networks, which have been proposed recently to alleviate the problem of inefficiently utilized spectrum by allowing cognitive devices to coexist with licensed users, given that the interference caused to the licensed users can be limited. The frequency bands used for DVB-T transmissions are a possible candidate for opportunistic spectrum access (OSA) [32], yet the harmonics created in that frequency band are known to coincide with the GPS L1 or Galileo E1 bands. As a consequence cognitive devices which are allowed to transmit in the UHF IV band when the digital television (DTV) broadcasting system is inactive, might create harmful interference to GNSS systems due to amplifiers' nonlinear behavior [33]. Although literature mentions different types of interference that can affect GNSS receivers, a theoretical framework that accounts for the effects of single and/or multiple sources of interference and for the channel fading affecting both SoI and interfering signals is still missing.

In this paper we develop a framework for the GNSS acquisition performance that accounts for a single interferer as well as for a network of interferers. The framework is flexible enough to jointly account for different channel conditions for the SoI and the interfering signals, as well as the spatial distribution and density of the interfering nodes. Moreover, the proposed framework provides the acquisition performance for different decision strategies. The acquisition performance is characterized by means of mathematical expressions of the probability of detection (P_d) and the probability of false alarm (P_{fa}). The resulting receiver operating characteristics (ROC) have been supported and validated by simulations. The main contributions of this work can be listed as follows: 1) the theoretical comparison of the most common acquisition methods, 2) the definition of a framework that allows to validate the acquisition performance for different channel conditions for the SoI and the interference, and 3) the adoption of aggregate network interference in the theoretical framework. The analytical framework for the acquisition performance of GNSS signals presented in this paper is of interest both for the correct setting of the detection threshold in realistic (future) signal conditions and for the definition of limit system parameters that guarantee a minimum required acquisition performance. Moreover, the framework can be used to plan where alternative localization systems should be deployed in order to achieve ubiquitous and accurate localization performance.

The remainder of the paper is organized as follows. In Section II the signal and system model is presented, introducing the assumptions that have been made. The search space is defined and the different acquisition strategies that have been studied are introduced. Section III analyzes the acquisition performance in the presence of a single interferer, while in Section IV the case of aggregate interference is discussed. Numerical results are presented in Section V. In Section VI the conclusions are drawn.

II. SIGNAL AND SYSTEM MODEL

In this section we introduce the signal and system model, as well as the decision strategies that are evaluated in the remainder of the paper.

A. Signal Model

After filtering and downconversion in the receiver front-end, the k-th sample of the received signal entering the acquisition block has the following form

$$s[k] = \sum_{l=1}^{N_{\text{sat}}} r_l[k] + i[k] + n[k] \tag{1}$$

where $s[k]$ is the sum of N_{sat} satellite signals $r_l[k]$, an interference term $i[k]$, and the noise term $n[k]$. We assume the noise samples to be independent and to follow a complex normal distribution $\mathcal{N}_c(0, N_0 f_s/2)$, with f_s the sampling frequency and N_0 the noise spectral density. The kth sample of the GNSS signal received from a single satellite can be represented as

$$r_l[k] = \sqrt{2P} H_l c_l[k - \tau_{c,l}] d_l[k - \tau_{c,l}] \cos[2\pi (f_{\text{IF}} + f_{d,l})k + \phi_l] \tag{2}$$

where P is the GNSS received signal power, H_l represents the fading affecting the lth satellite signal, c_l is the code with corresponding code phase $\tau_{c,l}$, f_{IF} and $f_{d,l}$ are the intermediate frequency and the Doppler frequency, and ϕ_l is the carrier phase error. For simplicity we suppose the data bit d_l to be 1. The main objective of the acquisition is

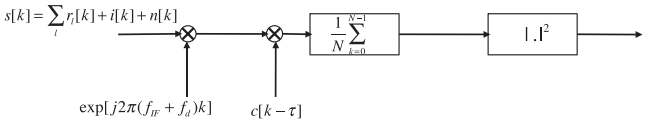

Fig. 1. Schematic of different processing steps for calculation of search space.

to determine the code phases $\tau_{c,1}, \tau_{c,2}, \cdots \tau_{c,N\text{sat}}$ and Doppler frequencies $f_{d,1}, f_{d,2}, \ldots, f_{d,N\text{sat}}$ of the satellites in view. Since the GPS L1 and Galileo E1 are operating in protected spectrum, we consider as source of interference the harmonics or intermodulation products of emissions in the UHF IV and UHF V frequency bands.[1]

B. System Model

The acquisition of GNSS signals is a classical detection problem where a signal impaired by noise and interference has to be identified. Prior to the tracking of GNSS signals, the receiver identifies which satellites can be used to determine a position and time solution and provides a rough estimation of the code phases and the Doppler frequencies of the present satellite signals. In the receiver acquisition block, the signal as defined in (1) is first downconverted to baseband. Subsequently, the downconverted signal is correlated with a local replica of the code and the correlator output is integrated over an interval which is an integer a times longer than the code period length N. As shown in Fig. 1, the unknown phase of the incoming signal is finally removed by taking the squared absolute value of the complex variable.

The acquisition process is a binary decision problem with two hypothesis. The $\mathcal{H}_1$ hypothesis corresponds to the scenario where the signal is present and correctly aligned with the local replica at the receiver. The null-hypothesis $\mathcal{H}_0$ corresponds to the case where the SoI is not present, or present but incorrectly aligned with the local replica. The acquisition performance is measured in terms of the probability of detection and the probability of false alarm. The probability of detection $\mathbb{P}_\text{d}$ is the probability that the decision variable V surpasses the threshold β in the presence of the SoI and can be expressed as $\mathbb{P}_\text{d}(\beta) = \mathbb{P}(V > \beta|\mathcal{H}_1)$. The probability of false alarm $\mathbb{P}_\text{fa}$ is the probability that V surpasses β in absence of SoI or when the signal is not correctly aligned with the local replica, and can be expressed as $\mathbb{P}_\text{fa}(\beta) = \mathbb{P}(V > \beta|\mathcal{H}_0)$.

In order to define the cell statistics, we characterize the different contributions to the cell values. The search space is discretized into different cells that correspond to possible values of the code phase and the Doppler frequency. The code phase $\tau_{c,l}$ of the different satellites in view are chosen from a finite set $\{\tau_{1,}\tau_{2,}\ldots,\tau_{aN}\}$ with $\tau_\text{p} = (p-1)\Delta\tau$, where we choose $\Delta\tau$ equal to the chip time T_c to allow a tractable analysis. As for the Doppler frequency, the value is chosen from the finite set $\{f_1, f_2, \ldots, f_L\}$, with $f_q = f_\text{min} + (q-1)\Delta f$, where the frequency resolution Δf and f_min are chosen according to the specifications of the application. Thus, we define the search space $\mathbf{X} \in \mathbb{R}^{aN\times L}$ where each cell cell $\mathbf{X}[p, q]$, $1 \le p \le aN$, $1 \le q \le L$ is given by

$$\begin{aligned}\mathbf{X}[p,q] &= \left|\frac{1}{aN}\sum_{k=1}^{aN}\left[\sum_{l=1}^{N_\text{sat}} r_l[k]+i[k]+n[k]\right]\right. \\ &\qquad \left.\times\, c[k-\tau_p]e^{j2\pi(f_\text{IF}+f_q)k}\right|^2 \\ &= |\mathbf{X}_\text{r}[p,q]+\mathbf{X}_\text{i}[p,q]+\mathbf{X}_\text{n}[p,q]|^2 \end{aligned} \quad (3)$$

with $\mathbf{X}_\text{r}[p, q]$, $\mathbf{X}_\text{i}[p, q]$, and $\mathbf{X}_\text{n}[p, q]$ the contributions of the satellite signals, the interference, and the noise, respectively.[2] The noise term $\mathbf{X}_\text{n}$ results from the downconversion and correlation with the local replica of the noise term in (1). The downconversion yields a complex Gaussian RV with variance of the real and the imaginary parts equal to $N_0 f_\text{s}/4$. The correlation with the local replica yields the mean value of N zero-mean, complex Gaussian RVs, and thus, $\mathbf{X}_\text{n} \sim \mathcal{N}_\text{c}(0, \sigma_\text{n}^2)$ with $\sigma_\text{n}^2 = N_0 f_\text{s}/(2N) = N_0/(2T_\text{per})$, where $T_\text{per} = NT_\text{c}$ is the code period. Note that in order to have independent noise samples, the sampling rate is $1/T_\text{c}$. We consider the term that originates from a single interferer after downconversion and despreading to be a Gaussian process, such that $\mathbf{X}_\text{i} \sim \mathcal{N}_\text{c}(0, \sigma_\text{i}^2)$. It is widely accepted that the Gaussian distribution is a good approximation for the interference in DSSS systems [34, 35]. When the Gaussian approximation of the contribution to the decision variable produced by the despreading of the interfering signal is not accurate, the proposed framework yields a pessimistic performance analysis [36]. In order to account for the interaction between the interfering signal and the despreading sequence, the spectral separation coefficient (SSC) is commonly used [37]. Since the contribution of the interference to the decision variable can be modeled as a Gaussian RV, and since the SSC values for complex white Gaussian noise are very similar for GPS C/A and Galileo BOC(1, 1) coding [14], the proposed theoretical model holds for a generic GNSS signal.

In this work we consider the Doppler frequency known and therefore, $\mathbf{X} \in \mathbb{R}^{aN\times L}$ reduces to a one-dimensional search space $\bar{X} \in \mathbb{R}^{aN}$ spanned over the set of code phase values. We refer to [38] for several acquisition techniques that include also the estimation of the Doppler frequency. For a known Doppler frequency, a cell of the search space $X[\tau] \in \bar{X}$ can be written as[3]

$$X[\tau] = \left|\sum_{l=1}^{N_\text{sat}} \sqrt{P}\, H_l R_l[\tau] e^{-j\phi_l} + X_\text{i}[\tau] + X_\text{n}[\tau]\right|^2 \quad (4)$$

[1] Our framework can be easily extended to the case of in-band (e.g. intentional) interference.

[2] In order to reduce notational complexity, without loss of generality we assume $a = 1$.

[3] To reduce the complexity of notation, the index p is further discarded.

where $R_l[\tau]$ is the cross-correlation function between the code under search and the code of the lth satellite. The contribution of interference and noise for the different code phase values is represented by $X_\mathrm{i} \in \mathbb{R}^{aN}$ and $X_\mathrm{n} \in \mathbb{R}^{aN}$, respectively. We consider the set of $\{H_l\}$ as independent and identically distributed (IID), with a constant value over the integration time and average fading power $\mathbb{E}\{H_l^2\} = 1$. Without loss of generality, let satellite 1 be the satellite under search. The value of a search space cell can now be expressed as

$$X[\tau] = \Bigg| \sqrt{P} H_1 R_1[\tau] e^{-j\phi_1} + \underbrace{\sum_{l=2}^{N_\mathrm{sat}} \sqrt{P} H_l R_l[\tau] e^{-j\phi_l}}_{X_\mathrm{c}[\tau]} + X_\mathrm{i}[\tau] + X_\mathrm{n}[\tau] \Bigg|^2 \quad (5)$$

where $X_\mathrm{c}[\tau]$ is the contribution of the cross-correlation noise to the value of a random search space cell. The distribution of $X_\mathrm{c}[\tau]$ can be well approximated by a complex, zero-mean Gaussian distributed RV [14]. The variance of $X_\mathrm{c}[\tau]$ can be written as

$$\sigma_\mathrm{c}^2 = [\mathbb{E}\{H_l^2\}(N_\mathrm{sat} - 1)P]\sigma_\mathrm{cross}^2/2 \quad (6)$$

where σ_cross^2 is the variance of the cross-correlation originating from a single satellite.

C. Decision Strategies

The acquisition performance does not only depend on the cell statistics, but also on the acquisition strategy that has been adopted. Different decision variables are commonly used, often on a heuristic basis. In general the goal of a decision strategy is to maximize the probability of detection and to minimize the probability of false alarm. In [2] the generalized likelihood ratio test (GLRT) is introduced. The GLRT leads to select the maximum of the search space defined as [5, 39]

$$V = \max\{\bar{X}\}. \quad (7)$$

The decision is then taken by comparing V with a threshold. In the GLRT strategy the Neyman-Pearson criterion is applied. For a selected probability of false alarm, a threshold that maximizes the probability of detection is chosen, such that the GLRT strategy is the optimal acquisition strategy when the signal conditions are perfectly known.

A second strategy to define a decision variable, called maximum ratio test (MRT), uses the ratio between the first and the second maximum of the search space [9, 40]

$$V = \frac{X_{(1)}}{X_{(2)}} \quad (8)$$

where $X_{(1)} \geq X_{(2)} \geq \ldots \geq X_{(aN-1)}$ are order statistics of $\bar{X}$.

III. SINGLE INTERFERER

In this section we consider the scenario where the interference stems from a single transmitter.

We propose an analytical approach for the evaluation of the acquisition performance that is based on the characteristic function (CF) of the decision variable. To define the statistics of the decision variable for this scenario, we analyze the contribution of the interference to the search space cell values. Although the interfering signal does not necessarily feature a zero-mean Gaussian distribution, it can be shown that the contribution to the decision variable produced by the despreading of the interfering signal can be often approximated by a Gaussian RV [34, 35]. As a case study we consider a DVB-T base-station as a single transmitter and the third harmonic of the DVB-T signal as the interference in the GNSS E1/L1 bands [33]. However, our approach can be used for several single interferer scenarios where both SoI and interferer are affected by fading. The contribution of the third harmonic of DVB-T to the different cells of the search space has been discussed in [14], and can be expressed as $X_\mathrm{i} \sim \mathcal{N}_\mathrm{c}(0, \sigma_\mathrm{i}^2)$. Therefore, the sum of the contributions stemming from the noise, the interference, and the cross-correlation can be merged to a single complex Gaussian RV.

$$X_\mathrm{IN} = X_\mathrm{c} + X_\mathrm{i} + X_\mathrm{n} \sim \mathcal{N}_\mathrm{c}(0, \sigma_\mathrm{tot}^2) \quad (9)$$

with $\sigma_\mathrm{tot}^2 = \sigma_\mathrm{c}^2 + \sigma_\mathrm{i}^2 + \sigma_\mathrm{n}^2$.

This completes the definition of the cell statistics and we proceed with the discussion of acquisition performance of the GLRT and MRT decision strategies.

A. Generalized Likelihood Ratio Test

1) The Probability of Detection: $\mathbb{P}_\mathrm{d}$ corresponds to the probability that the decision variable exceeds the threshold value in presence of the SoI. In the GLRT strategy the maximum value of the entire search space is selected as the decision variable. Let X_1 denote the cell value corresponding to the correct code phase, assumed without loss of generality to be τ_1, and let $\bar{X}_- = \bar{X} \backslash \{X_1\}$ denote the search space excluding cell X_1. Considering a relatively strong satellite signal power, we suppose that $X_1 = \max\{\bar{X}\} = X_{(1)}$. The RV X_1 can be written as

$$X_1 = |\sqrt{P} H_1 e^{-j\phi_1} + X_\mathrm{c}[\tau_1] + X_\mathrm{i}[\tau_1] + X_\mathrm{n}[\tau_1]|^2 \quad (10)$$

where we have considered the signal from satellite number 1 as the one under search.[4] When $X_1 = X_{(1)}$, the probability of detection can be found by applying the inversion theorem [41] and is given by

$$\mathbb{P}_\mathrm{d}(\beta | X_1 = X_{(1)}) = \mathbb{P}\{X_1 > \beta\} = \frac{1}{2} - \frac{1}{2\pi} \int_0^\infty \mathfrak{Re}\left\{ \frac{\psi_{X_1}(-j\omega) e^{j\omega\beta} - \psi_{X_1}(j\omega) e^{-j\omega\beta}}{j\omega} \right\} d\omega \quad (11)$$

where $\psi_{X_1}(j\omega)$ is the CF of the decision variable X_1. Conditioning on H_1, the RV X_1 follows a noncentral χ^2

[4] We consider the maximum of the auto-correlation equal to 1.

distribution with 2 degrees of freedom and noncentrality parameter $\mu_{X_1} = H_1^2 P$. The CF of X_1 conditioned on H_1 can be expressed as

$$\psi_{X_1|H_1}(j\omega) = \mathbb{E}\{e^{j\omega X_1|H_1}\} = \frac{1}{1-2j\omega\sigma_{\text{tot}}^2}\exp\left(\frac{j\omega H_1^2 P}{1-2j\omega\sigma_{\text{tot}}^2}\right). \quad (12)$$

Taking the expectation over H_1, (12) yields

$$\psi_{X_1}(j\omega) = \frac{1}{1-2j\omega\sigma_{\text{tot}}^2}\psi_{H_1^2}\left(\frac{j\omega P}{1-2j\omega\sigma_{\text{tot}}^2}\right). \quad (13)$$

where $\psi_{H_1^2}$ is the CF of the fading power. In case of Ricean or Rayleigh fading, the fading power features a noncentral chi-square and a central chi-square distribution, respectively. In both cases the CF is known in closed form. The Ricean distribution is frequently used for modeling outdoor channels [42], while the Rayleigh fading channel is used for modeling indoor channel environments [43].

To calculate $\mathbb{P}_{\text{d}}$ we supposed so far a strong signal power, which is made explicit in the conditions of (11). The signal missed-detection can however also occur when $X_1 \neq X_{(1)}$. In order to account for this case, we denote the maximum of the set of the incorrect code phase cell values as $X_2 = \max\{\bar{X}_-\}$, which follows a generalized exponential distribution [44].[5] The probability of detection is the result of the product of two probabilities, i.e., the detection probability of the cell corresponding to the correct code phase and the probability that the maximum of the rest of the search space is smaller than X_1 and therefore, $\mathbb{P}_{\text{d}}$ conditioned on H_1 can be expressed as

$$\mathbb{P}_{\text{d}}(\beta|H_1) = \mathbb{P}(X_{1|H_1} > \beta)\cdot\mathbb{P}(X_2 < X_{1|H_1}). \quad (14)$$

The two factors both are conditioned on the fading parameter h_1 and thus they are not independent. The probability of detection conditioned on H_1 can now be written as

$$\mathbb{P}_{\text{d}}(\beta|H_1) = \int_\beta^{+\infty}\int_0^x f_{X_2}(y) f_{X_1|H_1}(x)\,dy\,dx = \int_\beta^{+\infty} F_{X_2}(x) f_{X_1|H_1}(x)\,dx \quad (15)$$

where $F_{X_2}(x)$ is the cumulative distribution function (cdf) of a generalized exponential function. The cdf of the generalized exponential distribution can be expressed as [44]

$$F_{X_2}(x;\varrho,\zeta) = (1-e^{-\zeta x})^{\varrho}, \quad x > 0 \quad (16)$$

where $\varrho = N-1$ and $\zeta = 1/2\sigma_{\text{tot}}^2$ are the scale and shape parameters, respectively. In order to take into account the effect of the fading, we propose a unified approach based on the CF of X_1. Using the inversion theorem for the calculation of the probability density function (pdf) of X_1, the probability of detection can be expressed as

$$\mathbb{P}_{\text{d}}(\beta) = \frac{1}{\pi}\int_\beta^{+\infty} F_{X_2}(x) \times \int_0^{+\infty}\Re\mathfrak{e}\{\psi_{X_1}(j\omega)\exp(-j\omega x)\}d\omega dx. \quad (17)$$

By using the CF of X_1, we can easily include in the analysis the effect of fading on the SoI and on the interferer. The advantage of using the CF will become clear in the next section where we show that a double numerical integration will likewise allow us to calculate the probability of detection including the effects of fading and the effects of multiple interference instead of a recursive solution of nested integrations.

2) The probability of false alarm: $\mathbb{P}_{\text{fa}}$ corresponds to the probability that the decision variable exceeds the threshold value in absence of the signal. In this case the entire search space is composed of IID RVs following an exponential distribution. The probability that the decision variable exceeds the threshold can thus be written as follows

$$\mathbb{P}_{\text{fa}}(\beta) = 1 - F_{X_2}(\beta;N,\zeta) = 1-(1-e^{-\zeta\beta})^N. \quad (18)$$

REMARK. A third method proposed in [45] considers the decision variable defined as

$$V = \frac{X_{(1)}}{\sum_{X_k\in\bar{X}\setminus\{X_{(1)}\}} X_k/(N-1)}. \quad (19)$$

Since for a given value of the signal-to-noise ratio (SNR) and the signal-to-interference ratio (SIR), the value by which $X_{(1)}$ is scaled is a constant, the performance of this method is identical to the GLRT acquisition strategy. However, this method is beneficial since it inherently includes an estimation of the noise power, which is necessary to correctly set the threshold.

B. Maximum Ratio Test

For the MRT the decision variable is defined as the ratio of the highest correlation peak and the second highest correlation peak of the search space. This method is heuristic and has as the main advantage that $\mathbb{P}_{\text{fa}}$ is independent of the noise power density. This approach allows to set a fixed threshold corresponding to a selected false alarm rate, which is independent of the noise power [9].

1) Probability of Detection: As defined in Section III-A, let X_1 be the cell value corresponding to the correct code phase, and $X_2 = \max\{\bar{X}_-\}$. We assume a relatively strong satellite signal, such that $X_{(1)} = X_1$ and $X_{(2)} = X_2$. We can now rewrite (8) as

$$\tilde{V} = X_1 - \beta X_2. \quad (20)$$

When the SoI is present, X_1 can be expressed as in (10) and follows a noncentral chi-square distribution. Since the vector $\bar{X}_-$ is composed of IID RVs that follow an exponential distribution, X_2 follows a generalized exponential distribution. In the presence of the SoI, the

[5] We do not consider the contribution of the auto–correlation of the SoI that is present in all cells of $\bar{X}_-$, since it is negligible. Instead, we use σ_{tot}^2 as defined in (9).

acquisition of the GNSS signal is successful if $\tilde{V} > 0$. Therefore, by using the inversion theorem the probability of detection can be expressed as follows

$$\begin{aligned}\mathbb{P}_d(\beta) &= \mathbb{P}\left\{\tilde{V} > 0\right\} \\ &= \frac{1}{2} - \frac{1}{2\pi}\int_0^\infty \Re\mathfrak{e}\left\{\frac{\psi_{\tilde{V}}(-j\omega) - \psi_{\tilde{V}}(j\omega)}{j\omega}\right\} d\omega\end{aligned} \tag{21}$$

where $\psi_{\tilde{V}}(j\omega)$ is the CF of the variable $\tilde{V}$. For a given threshold value β, the CF of the decision variable is given by

$$\psi_{\tilde{V}}(j\omega) = \mathbb{E}\left\{e^{j\omega\tilde{V}}\right\} = \mathbb{E}\{e^{j\omega(X_1 - \beta X_2)}\}. \tag{22}$$

Since X_1 and X_2 are independent RVs, the CF of $\tilde{V}$ can be written as

$$\psi_{\tilde{V}}(j\omega) = \frac{1}{1 - 2j\omega\sigma_{\text{tot}}^2}\psi_{H_1^2}\left(\frac{j\omega P}{1 - 2j\omega\sigma_{\text{tot}}^2}\right)\psi_{X_2}(-j\omega\beta). \tag{23}$$

Since X_2 follows a generalized exponential distribution, the CF of X_2 can be written in closed form as [44]

$$\psi_{X_2}(j\omega) = \frac{\Gamma(N)\Gamma(1 - \frac{j\omega}{\zeta})}{\Gamma(N - \frac{j\omega}{\zeta})}. \tag{24}$$

Unfortunately, the CF of X_2 is not in a convenient form for numerical integration, since the Gamma function diverges to infinity in the integration interval of (21). However, recently the generalized exponential function has been demonstrated to provide a good approximation of the Gamma distribution [46]. Therefore, we approximate the distribution of the generalized exponential RV with a Gamma distribution defined by the two parameters k and θ. In order to estimate the parameters of the Gamma distribution, we use the method of the moments by imposing the equivalence of the first two moments of the Gamma distribution with the first two moments of X_2. Since mean and variance of the Gamma distribution are expressed as

$$\mu_G = k\theta \text{ and } \sigma_G^2 = k\theta^2 \tag{25}$$

and for X_2 we have

$$\mu_{X_2} = \frac{1}{\zeta}[\eta(N) - \eta(1)] \quad \text{and} \quad \sigma_{X_2}^2 = \frac{1}{\zeta^2}[\eta'(1) - \eta'(N)] \tag{26}$$

the parameters of the Gamma distribution can be expressed as

$$\theta = \frac{1}{\zeta}\frac{\eta'(1) - \eta'(N)}{\eta(N) - \eta(1)} \tag{27}$$

and

$$k = \frac{[\eta(N) - \eta(1)]^2}{\eta'(1) - \eta'(N)} \tag{28}$$

where $\eta(x)$ and $\eta'(x)$ are the digamma and the polygamma function, respectively. Finally, the CF of the decision variable $\tilde{V}$ can be obtained by inserting the CF of the Gamma distributed RV X_2 in (23)

$$\psi_{\tilde{V}}(j\omega) = \frac{1}{1-2j\omega\sigma_{\text{tot}}^2}\psi_{H_1^2}\left(\frac{j\omega P}{1-2j\omega\sigma_{\text{tot}}^2}\right)(1+j\omega\beta\theta)^{-k}. \tag{29}$$

The probability of detection can be calculated by substituting (29) in (21). Note that in the GLRT strategy a second numerical integration is necessary to account for the probability that the cell corresponding to the correct code phase does not correspond to the maximum of the search space. Differently, the MRT strategy inherently accounts for this probability, i.e., the MRT strategy depends upon the probability distribution of the two independent RVs X_1 and X_2 and therefore, contains the probability that X_2 exceeds X_1. Moreover, only a single numerical integration is needed.

2) The Probability of False Alarm: $\mathbb{P}_{\text{fa}}$ has been derived analytically in [47]. According to the theory of order statistics, $\mathbb{P}_{\text{fa}}$ can be written as

$$\mathbb{P}_{\text{fa}}(\beta) = (N^2 - N)\mathcal{B}(N - 1, 1 + \beta) \tag{30}$$

where $\mathcal{B}$ is the Beta function.

IV. AGGREGATE INTERFERENCE

The scenario where the interference stems from a network of interferers is of increasing importance, as reported in recent literature [48–50]. In this section we consider multiple interferers scattered over the plane according to a homogeneous Poisson point process (PPP). It is known that for this scenario the approximation of the multiple interference by a Gaussian process is very poor. The aggregate network interference can rather be modeled as an α-stable process, where the characteristic exponent of the process is a function of the path-loss exponent, and the dispersion is affected by the channel randomness. We present a statistical model of aggregate interference that was proposed in [51] and [48], and we analyze the impact of this type of interference on the acquisition of the satellite signal for the GLRT acquisition strategy.

A. Interference Modeling

As discussed in Section III, the correlation of a single interferer with the local replica of the code yields a complex Gaussian contribution to the decision variable. When we consider a network of interferers, we apply a stochastic geometry approach to capture the randomness of the topology and model the spatial distribution of the interferer locations according to a homogeneous PPP [49]. The probability that k interferers lie inside region $\mathcal{R}$ depends on the spatial density of the interfering nodes λ and the area $A_{\mathcal{R}}$ of the region $\mathcal{R}$, and can be written as [52]

$$\mathbb{P}\{k \in \mathcal{R}\} = \frac{(\lambda A_{\mathcal{R}})^k}{k!}e^{-\lambda A_{\mathcal{R}}}. \tag{31}$$

Without loss of generality we consider the receiver located at the origin of an infinite plane,[6] and we express the aggregate interference measured at the origin as

$$X_{\mathrm{i}} = \sum_{m=1}^{\infty} I_m. \tag{32}$$

The m-th interfering signal in (32) can be written as

$$I_m = \frac{1}{R_m^v} G_m \left(I_{m,1} + j I_{m,2} \right) \tag{33}$$

where $I_{m,1}$ and $I_{m,2}$ are two IID Gaussian RVs with zero mean and variance $\sigma_{\mathrm{i}}^2/2$. The term σ_{i}^2 represents the interferer transmission power at a distance of 1 m (far-field assumption) in the affected GNSS band. The RV G_m represents the fading that affects the m-th interferer. As in the far-field, the signal power decays with $1/R_m^{2v}$, where R_m is the distance of node m with respect to the victim receiver and v is the amplitude path–loss exponent. It is worth to notice that since $I_{m,1}$ and $I_{m,2}$ are two IID Gaussian RVs with mean equal to zero, I_m is circular symmetric (CS). We suppose that there is no coordination between the different transmitters and thus they transmit asynchronously and independently. Under such conditions it can be shown that X_{i} follows a symmetric stable distribution [48, 49, 52–54]

$$X_{\mathrm{i}} \sim \mathcal{S}_{\mathrm{c}}(\alpha = 2/v, \beta = 0, \gamma = \pi \lambda C_{2/v}^{-1} \mathbb{E}\{|G_m I_{m,p}|^{2/v}\}) \tag{34}$$

with $C_x = \frac{1-x}{\Gamma(2-x)\cos(\pi x/2)}$. The characteristic exponent α depends on the path-loss exponent, while the dispersion γ is a function of the channel fading parameter, the interferer node density, and the interferer transmission power.

B. Acquisition Performance in the Presence of Aggregate Interference

In the presence of aggregate interference, the decision variable can be expressed as

$$X_1 = |\underbrace{\sqrt{P} H e^{-j\phi} + X_{\mathrm{i}}}_{M} + X_{\mathrm{c}} + X_{\mathrm{n}}|^2 \tag{35}$$

where M stands for the contribution to the decision variable of the SoI and the aggregate interference. The sum of the noise and cross-correlation noise is a Gaussian RV with variance $\sigma_{\mathrm{nc}}^2 = \sigma_{\mathrm{n}}^2 + \sigma_{\mathrm{c}}^2$. Conditioning on M, X_1 follows a noncentral chi-square distribution with two degrees of freedom $X_1 \sim \chi_{\mathrm{nc}}^2(M^2, \sigma_{\mathrm{nc}}^2)$, where M^2 represents the noncentrality term. The CF of X_1 conditioned on M can be written as

$$\psi_{X_1|M}(j\omega) = \frac{1}{1 - 2j\omega\sigma_{\mathrm{nc}}^2} \exp\left(\frac{j\omega M^2}{1 - 2j\omega\sigma_{\mathrm{nc}}^2} \right). \tag{36}$$

By taking the expectation over M, the CF of X_1 can be expressed as

$$\psi_{X_1}(j\omega) = \frac{1}{1 - 2j\omega\sigma_{\mathrm{nc}}^2} \psi_{M^2}\left(\frac{j\omega}{1 - 2j\omega\sigma_{\mathrm{nc}}^2} \right). \tag{37}$$

1) Rayleigh Fading for the SoI: We now consider the case of H distributed according to the Rayleigh distribution. Conditioning on X_{i}, M^2 follows a noncentral chi-square distribution with two degrees of freedom $M_{|X_{\mathrm{i}}}^2 \sim \chi_{\mathrm{nc}}^2\left(X_{\mathrm{i}}^2, P\sigma_H^2\right)$. Therefore, the CF of M^2 conditioned on X_{i} can be written as

$$\psi_{M^2|X_{\mathrm{i}}}(j\omega) = \frac{1}{1 - 2j\omega P\sigma_H^2} \exp\left(\frac{j\omega X_{\mathrm{i}}^2}{1 - 2j\omega P\sigma_H^2} \right) \tag{38}$$

with $\sigma_H^2 = 1/2$. By inserting (38) in (37), the CF of X_1 conditioned on X_{i} can be expressed as follows

$$\psi_{X_1|X_{\mathrm{i}}}(j\omega) = \frac{1}{1-2j\omega(P/2+\sigma_{\mathrm{nc}}^2)} \exp\left(\frac{j\omega X_{\mathrm{i}}^2}{1-2j\omega(P/2\sigma_{\mathrm{nc}}^2)} \right). \tag{39}$$

By taking the expectation over X_{i}, the CF of the decision variable can be expressed as

$$\psi_{X_1}(j\omega) = \frac{1}{1-2j\omega(P/2+\sigma_{\mathrm{nc}}^2)} \psi_{X_{\mathrm{i}}^2}\left(\frac{j\omega}{1-2j\omega(P/2\sigma_{\mathrm{nc}}^2)} \right). \tag{40}$$

Consider a symmetric stable distribution $X \sim \mathcal{S}(\alpha, 0, \gamma)$, then X can be decomposed as $X = \sqrt{U}G$, where $U \sim \mathcal{S}(\alpha/2, 1, \cos(\pi\alpha/4))$ and $G \sim \mathcal{N}_{\mathrm{c}}(0, 2\gamma^{2/\alpha})$, with U and G independent RVs [53]. By using the decomposition property of symmetric stable distributions, the aggregate interference term can be written as $X_{\mathrm{i}} = \sqrt{U}G$. Therefore, the square of the aggregate interference can be expressed as

$$X_{\mathrm{i}}^2 = 2\gamma^v UC \tag{41}$$

where C is a central chi-square RV with two degrees of freedom. Conditioning on C and using the scaling property of a stable RV,[7] X_{i}^2 conditioned on C follows a stable distribution and therefore, the CF of X_{i}^2 conditioned on C is given by

$$\psi_{X_{\mathrm{i}}^2|C}(j\omega) = \exp\left\{ -(2C)^{1/v}\gamma \cos\left(\frac{\pi}{2v}\right)|j\omega|^{1/v} \times \left[1 - \mathrm{sign}(j\omega)\tan\left(\frac{\pi}{2v}\right)\right]\right\}. \tag{42}$$

The RV $C^{1/v}$ can be approximated by a Gamma RV Z [54]. By taking the expectation over Z, we can express the CF of X_{i}^2 as

$$\psi_{X_{\mathrm{i}}^2}(j\omega) = \left(1 + \theta_v 2^{1/v}\gamma \cos\left(\frac{\pi}{2v}\right)|j\omega|^{1/v} \times \left[1 - \mathrm{sign}(j\omega)\tan\left(\frac{\pi}{2v}\right)\right]\right)^{-k_v}. \tag{43}$$

[6] Although the interferers are distributed over an infinite plane, only the nearest interferers have a substantial contribution to the aggregate interference.

[7] If $X \sim \mathcal{S}(\alpha, \beta, \gamma)$ then $kX \sim \mathcal{S}(\alpha, \mathrm{sign}(k)\beta, |k|^{\alpha}\gamma)$

Note that the first and second moment of $C^{1/v}$ can be expressed as $2^{1/v}\Gamma\left(\frac{N}{2}+\frac{1}{v}\right)/\Gamma\left(\frac{N}{2}\right)$ and $4^{1/v}\Gamma\left(\frac{N}{2}+\frac{2}{v}\right)/\Gamma\left(\frac{N}{2}\right)$. Similarly to what we have done in Section III-B.1, the shape parameter $k^{1/v}$ and the scale parameter $\theta^{1/v}$ of the Gamma RV Z can be found by applying the method of moments. By using (43) and (40), the closed-form expression of the CF of X_1 can be written as

$$\psi_{X_1}(j\omega) = \frac{1}{1-2j\omega(P/2+\sigma_{\text{nc}}^2)}\left\{1+\theta_v 2^{1/v}\gamma\cos\left(\frac{\pi}{2v}\right)\times\left|\frac{j\omega}{1-2j\omega(P/2+\sigma_{\text{nc}}^2)}\right|^{1/v}\times\left[1-\text{sign}\left(\frac{j\omega}{1-2j\omega(P/2+\sigma_{\text{nc}}^2)}\right)\tan\left(\frac{\pi}{2v}\right)\right]\right\}^{-k_v}. \quad (44)$$

Note that when λ tends to zero (i.e. the dispersion γ tends to zero), (44) reduces to the scenario without interference where the SoI is subject to a Rayleigh fading channel. Inserting (44) in (17), $\mathbb{P}_{\text{d}}$ can be obtained. Note that for the scenario of aggregate interference the methodology to calculate $\mathbb{P}_{\text{d}}$ based on the CF requires a double integration, whereas the methodology based on the pdf requires a series of nested integrations in order to average over all RVs.

2) Ricean Fading for the SoI: For H that follows a Ricean distribution, we cannot obtain a closed-form expression of the CF. However, using the decomposition property for symmetric stable distributions, X_{i} can be expressed as $X_{\text{i}} = \sqrt{U}G$ with U and G defined as in Section IV-B.l. Therefore, conditioning on U, we find now that [49]

$$(X_{\text{i}} + X_{\text{n}} + X_{\text{n}})_{|U} \sim \mathcal{N}_{\text{c}}(0, \sigma_{\text{nc}}^2 + U2\gamma^{2/\alpha}) \quad (45)$$

which is analogue to (9) where only one interferer is present. The framework reduces to the single interferer case and $\mathbb{P}_{\text{d}}$ conditioned on U can be found by (17). $\mathbb{P}_{\text{d}}$ can be derived by numerically averaging over a large set of realizations of U.

C. False Alarm Probability

A cell of the search space with no SoI can be expressed as $X[\tau] = |X_{\text{i}}[\tau] + X_{\text{c}}[\tau] + X_{\text{n}}[\tau]|^2$. The contribution of the aggregate interference to the search space can be represented by a vector $\bar{X}_{\text{i}}$ composed of aN elements. Since $\bar{X}_{\text{i}}$ is a multivariate symmetric stable RV, the vector can be decomposed as

$$\bar{X}_{\text{i}} = \sqrt{U}\bar{G} \quad (46)$$

where $U \sim \mathcal{S}(\alpha/2, 1, \cos(\pi\alpha/4))$ and $\bar{G}$ is an aN-dimensional Gaussian random vector with $\bar{G} \sim \mathcal{N}_{\text{c}}(0, 2\gamma^{2/\alpha})$. Conditioning on U, for each cell of the search space where no SoI is present we have

$$X_{\text{i}}[\tau] \sim \mathcal{N}_{\text{c}}(0, U2\gamma^{2/\alpha}). \quad (47)$$

Therefore, the cell values of the search space have contributions from three Gaussian RV's X_{n}, X_{c}, and $X_{\text{i}|U}$. Once again, the framework is equivalent to the scenario of a single interferer and the $\mathbb{P}_{\text{fa}}$ conditioned on U can be calculated using (18). The $\mathbb{P}_{\text{fa}}$ can be obtained by averaging over a large set of realizations of the stable distribution U.

Note on independence: The vector $\bar{X}_{\text{i}}$ is given by

$$\bar{X}_{\text{i}} = \sum_{m=1}^{\infty}\frac{G_m}{R_m^v}\bar{I}_m \quad (48)$$

where $\bar{I}_m$ is a vector of uncorrected complex Gaussian RVs. From (48) we can conclude that the components of $\bar{X}_{\text{i}}$ are identically distributed, yet mutually dependent. Bearing in mind that the elements of $\bar{X}_{\text{i}}$ are not independent, the search space cell that contains the SoI is not independent of the rest of the search space. For the scenario of Rayleigh fading affecting the SoI, $\mathbb{P}_{\text{fa}}$ is calculated using a set of realizations of the aggregate interference, while $\mathbb{P}_{\text{d}}$ is calculated based on the closed-form expression of the CF of the decision variable, thus neglecting the dependence of the search space cell containing the SoI and the rest of the search space. It can be shown through simulation that this approximation is accurate.

V. NUMERICAL RESULTS

In this section we evaluate the acquisition performance using the expressions developed in Section III and in Section IV.

A. Single Interferer

In order to test the validity of the analytical model for the GLRT detection strategy, we compare the ROC curves obtained using the analytical expressions given in (17) and (18) with the simulation result obtained with the Monte Carlo method. In the simulator environment the signals are created in baseband where the acquisition is implemented according to Fig. 1. In each simulation we assume 8 random satellites to be in view, and we consider the same fading distributions as for the theoretical analysis. The DVB-T interference has been implemented as the third harmonic of a complex Gaussian signal. In the single interferer scenario 10^4 simulations are performed. The simulation parameters are summarized in Table I.

TABLE I
Simulation Parameters

Sampling frequency	1.023MHz
Intermediate frequency	0
Number of samples per chip	1
Code length	1023
Modulation	BPSK
SNR (postcorrelation)	15 dB
SIR (postcorrelation, single interferer)	15-30 dB
Number of simulations	10^4
INR (postcorrelation)	0-15 dB
λ	0.001 – 0.02m/s^2
Realizations aggregate interference	10^6

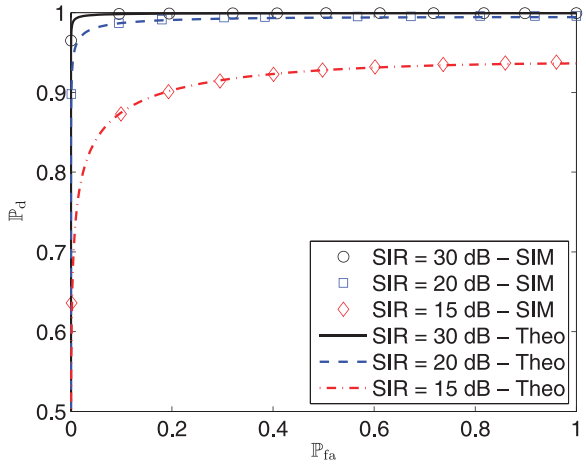

Fig. 2. ROC curves for GLRT acquisition strategy by simulation (markers) and theoretical analysis (lines) for SNR = 15 dB.

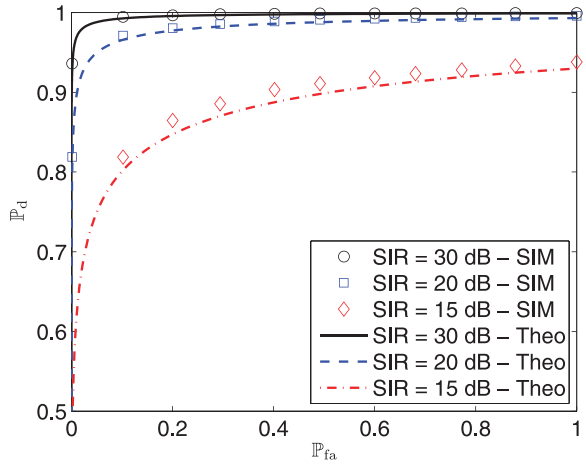

Fig. 3. ROC curves for GLRT acquisition strategy by simulation (markers) and theoretical analysis (lines) for SNR = 15 dB.

Fig. 2 shows the ROC curves of the GLRT for several values of the SIR.[8] Analytical results are indicated by lines, while markers represent the simulation results. The good agreement between the numerical and simulation results validates the proposed theoretical model for the GLRT. Fig. 3 shows the ROC curves of the MRT detection strategy for several SIR values where the simulation results are indicated by markers. The figure shows a minor offset between the theoretical model and the simulation results, in particular for low values of the SIR. This effect is due to the approximation of the generalized exponential distribution using the Gamma distribution.

In Fig. 4 the performance of the GLRT and the MRT decision strategies are compared for the single interferer case in the absence of fading. Fig. 4 reflects the optimality of GLRT in the absence of fading and under perfect

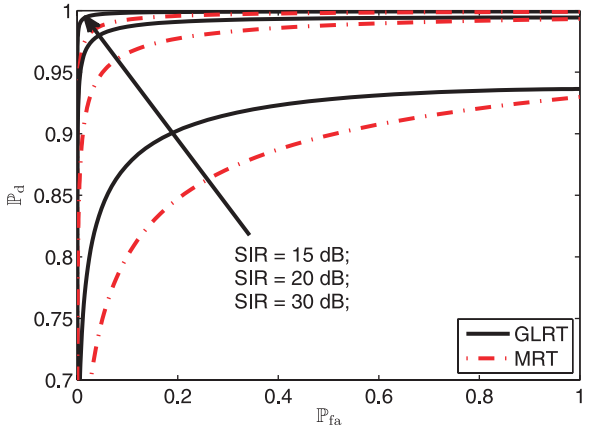

Fig. 4. Analytical ROC curves for GLRT and MRT (SNR = 15 dB).

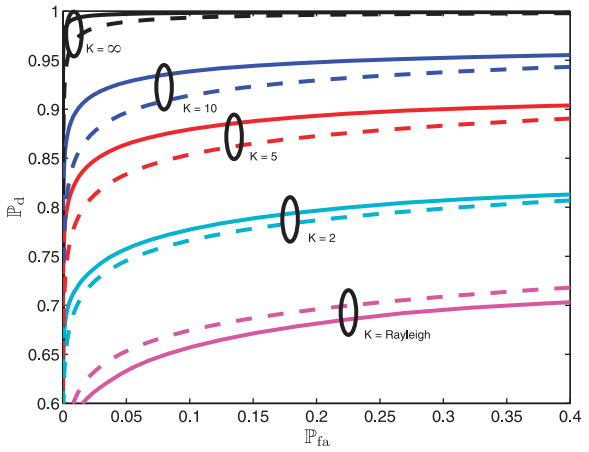

Fig. 5. Impact of K on ROC curves is represented, where fading is considered relative to SoI for GLRT (solid lines) and MRT (dashed lines). SNR = 15 dB and SIR = 30 dB.

synchronization.[9] As illustrated in the figure, the proposed framework allows us to quantify how much the GLRT method outperforms the MRT strategy. Note that this justifies why in Section IV only the GLRT method has been analysed.

Although this framework provides an analytical tool that allows us to include simultaneously the effect of fading on both SoI and interference, we only consider fading affecting either the SoI or the interference. We first analyze the effect of Ricean fading which is typical in urban environment. Ricean fading is characterized by the parameter K, representing the ratio between the energy of the line-of-sight (LOS) component and the energy of the other multipath components. Fig. 5 illustrates the effect on the acquisition performance of fading relative to the GNSS signal. From this figure we can notice that the acquisition performance decreases with decreasing values of K. Interestingly, the gap between the performance of GLRT and MRT diminishes with decreasing K until the

[8]Note that we define both the SNR and the SIR for the decision variable, i.e., after the correlation with the local replica of the code.

[9]In such conditions the GLRT reduces to the likelihood ratio test (LRT), which is optimal due to the Neyman-Pearson theorem [2].

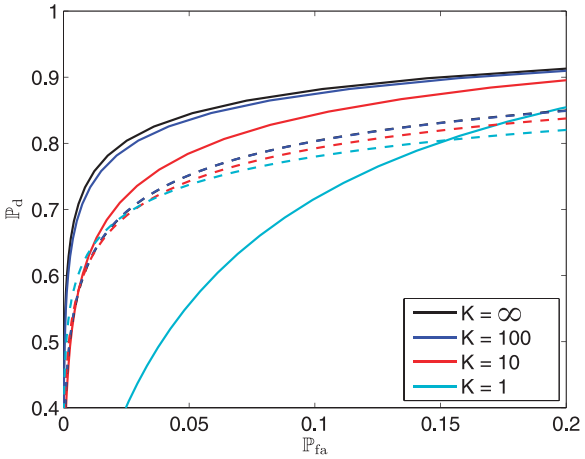

Fig. 6. Impact on ROC curves of Ricean fading relative to interfering signal is represented as function of Ricean factor K for GLRT acquisition strategy (solid lines) and MRT acquisition strategy (dashed lines). SNR = 15 dB and SIR = 15 dB.

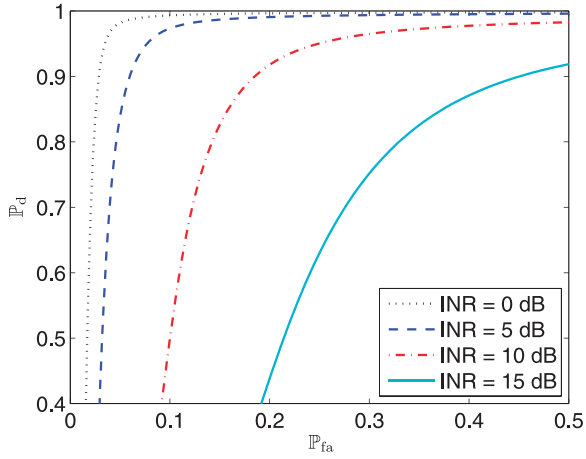

Fig. 7. ROC curves for GLRT method (SNR = 15 dB, $K = \infty$, and $\lambda = 0.01/\text{m}^2$) for varying values of INR.

point where MRT outperforms GLRT for $K = 0$. This is due to the fact that when fading affects the SoI, GLRT is not optimal anymore. From the numerical result presented in Fig. 5, we can conclude that MRT is more robust than GLRT in severe fading conditions. Fig. 6 compares the acquisition performance of the GLRT and MRT acquisition strategies with different fading distributions relative to the interference. In order to better understand the effect of the interference, we select SIR = 15 dB which corresponds to a powerful interferer. While for high values of K GLRT outperforms MRT, we notice that MRT is clearly more robust than GLRT when the interference is subject to fading. Considering that for the MRT acquisition strategy both X_1 and X_2 contain contributions from the interference, it can be understood that the effect of the fading affecting the interference is partially cancelled by taking the ratio of X_1 and X_2.

B. Aggregate Interference

In Section IV we presented analytical and semianalytical methods to determine the ROC curves corresponding to the GLRT acquisition strategy in the presence of aggregate interference. The obtained results include the effect of the spatial distribution of the interfering nodes and the transmission characteristics of both SoI and interference. In order to reduce the number of scenarios, we only consider Rayleigh fading for the interfering nodes which is realistic in challenging channel conditions, while for the SoI different fading distributions are considered. For simulation of the aggregate interference, 10^6 realizations of the stable RV have been generated.

Fig. 7 illustrates the effect of the transmission power of the cognitive devices on the ROC curves for a constant value of K. For interference-to-noise ratio (INR) = 15 dB, the reduction of the acquisition performance is considerable. Fig. 8 demonstrates the effect of different

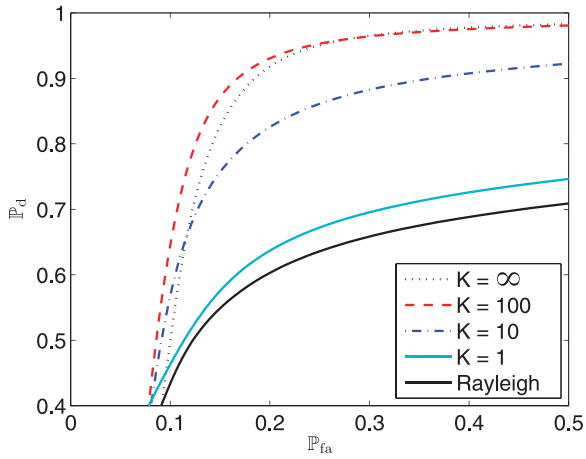

Fig. 8. ROC curves for GLRT method in presence of network of spatially distributed cognitive devices (SNR = 15 dB, INR = 5 dB, $\lambda = 0.01/\text{m}^2$, and $v = 1.5$). Impact of fading distribution (Ricean and Rayleigh) with regard to SoI is considered.

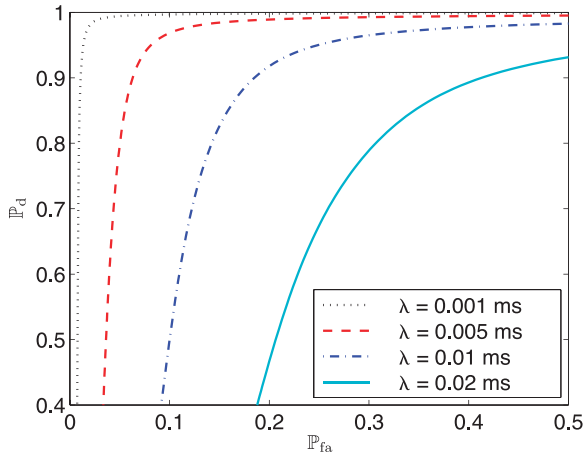

Fig. 9. ROC curves for GLRT method (SNR = 15 dB, $K = 10$, and INR = 10 dB), in Ricean fading channel for varying λ.

types of fading relative to the SoI. As expected, for higher values of K (stronger LOS), the ROC curve approaches the acquisition performance when there is no fading on the SoI. In Fig. 9 we show the effect of the interferer density on the acquisition performance. We can notice that the performance deteriorates quickly with increasing interferer density.

VI. CONCLUSIONS

In this paper we analyze the acquisition performance of GNSS signals in realistic urban scenarios, challenged by the presence of interference. We derive analytical expressions of the detection and false alarm probability that account for different acquisition strategies, single and multiple interferers, and different channel conditions. For the single interferer case, we analyze both the GLRT and the MRT strategy and show the effects of the channel fading on both the SoI and the interference. Further, we characterize the interference originating from spatially scattered interfering devices. For the multiple interference case, we analyze the acquisition performance of the GLRT acquisition strategy. The expressions for the probability of detection and false alarm account for network parameters such as the interferer node density, the transmission power of the nodes, and the fading distribution for the interference and the signal of interest. The analytical framework proposed in this paper allows us to understand the effect of several environment related parameters on the acquisition performance of the GNSS signal. Therefore, the frame-work can be used both to determine threshold values for the discussed network parameters corresponding to a minimum acquisition performance, and to plan the deployment of alternative localization systems to guarantee ubiquitous and accurate positioning performance.

REFERENCES

[1] Goldsmith, A.
Wireless Communications. New York: Cambridge University Press, 2005.

[2] VanTrees, H. L.
Detection, Estimation, and Modulation Theory - Part 1. New York: Wiley, 2001.

[3] Borio, D.
A statistical theory for GNSS signal acquisition. PhD thesis, Politecnico di Torino, Italy, Mar. 2008.

[4] Polydoros, A. and Weber, C. L.
A unified approach to serial search spread-spectrum code acquisition - Part I: General theory.
IEEE Transactions on Communications, **32**, 5 (May 1984), 542–549.

[5] Corazza, G. E.
On the MAX/TC criterion for code acquisition and its application to DS-SSMA systems.
IEEE Transactions on Communications, **44**, 9 (Sept. 1996), 1173–1182.

[6] Iinatti, J. H. J.
On the threshold setting principles in code acquisition of DS-SS signals.
IEEE Journal on Selected Areas in Communications, **18**, 1 (Jan. 2000), 62–72.

[7] Katz, M. D., Iinatti, J. H. J., and Glisic, S.
Two-dimensional code acquisition in time and angular domains.
IEEE Journal on Selected Areas in Communications, **19**, 12 (Dec. 2001), 2441–2451.

[8] Chiani, M. and Martini, M. G.
Analysis of optimum frame synchronization based on periodically embedded sync words.
IEEE Transactions on Communications, **55**, 11 (Nov. 2007), 2056–2060.

[9] Akos, D. M. et al.
Low power Global Navigation Satellite System (GNSS) signal detection and processing.
In *Proceedings of the ION GPS Conference*, Salt Lake City, UT, Sept. 2000, pp. 784–791.

[10] Borio, D.
GNSS acquisition in the presence of continuous wave interference.
IEEE Transactions on Aerospace and Electronic Systems, **46**, 1 (Jan. 2010), 47–60.

[11] Balaei, A. T., Dempster, A. G., and Lo Presti, L.
Characterization of the effects of CW and pulse CW interference on the GPS signal quality.
IEEE Transactions on Aerospace and Electronic Systems, **45**, 4 (Oct. 2009).

[12] Bastide, F. et al.
GPS L5 and Galileo E5a/E5b signal-to-noise density ratio degradation due to DME/TACAN signals: Simulations and theoretical derivation.
In *Proceedings of the 2004 National Technical Meeting of The Institute of Navigation*, San Diego, CA, Jan. 2004, pp. 1049–1062.

[13] Borio, D., Savasta, S., and Lo Presti, L.
On the DVB-T coexistence with Galileo and GPS system.
In *Proceedings of the 3rd ESA Workshop on Satellite Navigation User Equipment Technologies (NAVITEC)*, Noordwijk, the Netherlands, Dec. 2006.

[14] Wildemeersch, M. et al.
Interference assessment of DVB-T within the GPS LI and Galileo El Band.
In *Proceedings of the 5th ESA Workshop on Satellite Navigation Technologies and European Workshop on GNSS Signals and Signal Processing (NAVITEC)*, Noordwijk, the Netherlands, Dec. 2010.

[15] Sourour, E. A. and Gupta, S. C.
Direct-sequence spread-spectrum parallel acquisition in a fading mobile channel.
IEEE Transactions on Communications, **38**, 7 (July 1990), 992–998.

[16] Corazza, G. E. et al.
DS-CDMA code acquisition in the presence of correlated fading - Part I: Theoretical aspects.
IEEE Transactions on Communications, **52**, 7 (July 2004), 1160–1168.

[17] Caini, C., Corazza, G. E., and Vanelli-Coralli, A.
DS-CDMA code acquisition in the presence of correlated fading—Part II: Application to cellular networks.
IEEE Transactions on Communications, **52**, 8 (Aug. 2004), 1397–1407.

[18] Rick, R. R. and Milstein, L. B.
Parallel acquisition in mobile DS-CDMA systems.
IEEE Transactions on Communications, **45**, 11 (Nov. 1997), 1466–1476.

[19] Rick, R. R. and Milstein, L. B.
Optimal decision strategies for acquisition of spread-spectrum signals in frequency-selective fading channels.
IEEE Transactions on Communications, **46**, 5 (May 1998), 686–694.

[20] Suwansantisuk, W., Win, M. Z., and Shepp, L. A.
On the performance of wide-bandwidth signal acquisition in dense multipath channels.
IEEE Transactions on Vehicular Technology, **54**, 5 (Sept. 2005), 1584–1594.

[21] Suwansantisuk, W. and Win, M. Z.
Multipath aided rapid acquisition: Optimal search strategies.
IEEE Transactions on Information Theory, **53**, 1 (Jan. 2007), 174–193.

[22] Suwansantisuk, W., Chiani, M., and Win, M. Z.
Frame synchronization for variable-length packets.
IEEE Journal on Selected Areas in Communications, **26**, 1 (Jan. 2008), 52–69.

[23] Motella, B. et al.
Method for assessing the interference impact on GNSS receivers.
IEEE Transactions on Aerospace and Electronic Systems, **47**, 2 (Apr. 2011), 1416–1432.

[24] Lopez-Perez, D. et al.
Enhanced intercell interference coordination challenges in heterogeneous networks.
IEEE Wireless Communications, **18**, 3 (June 2011), 22–30.

[25] Betz, J. W. and Titus, B. M.
Intersystem and intrasystem interference with signal imperfections.
In *Proceedings of IEEE Position Location and Navigation Symposium (PLANS)*, San Diego, CA, Apr. 2006, pp. 558–565.

[26] Martin, S., Kuhlen, H., and Abt, T.
Interference and regulatory aspects of GNSS pseudolites.
Journal of Global Positioning Systems, **6**, 2 (2007), 98–107.

[27] Regulatory framework for indoor GNSS pseudolites. Technical Report ECC Report 168, ECC-CEPT, 2011.

[28] Borio, D., O'Driscoll, C., and Fortuny-Guasch, J.
Pulsed pseudolite signal effects on non-participating GNSS receivers.
In *IEEE International Conference on Indoor Positioning and Indoor Navigation (IPIN)*, Guimaraes, Portugal, Sept. 2011, pp. 1–6.

[29] Anderson, D. S. et al.
Assessment of compatibility between ultrawideband (UWB) systems and Global Positioning System (GPS) receivers.
Technical Report 01-45, NTIA, 2001.

[30] Van Slyke, T., Kuhn, W. B., and Natarajan, B.
Measuring interference from a UWB transmitter in the GPS LI band.
In *IEEE Radio and Wireless Symposium (RWS)*, Orlando, Fl, Jan. 2008, pp. 887–890.

[31] Peterson, K. M. and Erlandson, R. J.
Analytic statistical model for aggregate radio frequency interference to airborne GPS receivers from ground-based emitters.
Navigation, **59**, 1 (Spring 2012), 25–35.

[32] Goh, L. P., Lei, Z., and Chin, F.
DVB detector for cognitive radio.
In *Proceedings of IEEE International Conference on Communications*, Glasgow, Scotland, June 2007, pp. 6460–6465.

[33] Motella, B., Pini, M., and Dovis, F.
Investigation on the effect of strong out-of-band signals on Global Navigation Satellite Systems receivers.
GPS Solutions, **12**, 2 (2008), 77–86.

[34] Giorgetti, A. and Chiani, M.
Influence of fading on the Gaussian approximation for BPSK and QPSK with asynchronous cochannel interference.
IEEE Transactions on Wireless Communications, **4**, 2 (Mar. 2005), 384–389.

[35] Giorgetti, A., Chiani, M., and Win, M. Z.
The effect of narrowband interference on wideband wireless communication systems.
IEEE Transactions on Communications, **53**, 12 (Dec. 2005), 2139–2149.

[36] Dardari, D. and Pasolini, G.
Simple and accurate models for error probability evaluation of IEEE 802.11 DS SS physical interface in the presence of Bluetooth interference.
In *Proceedings of IEEE Global Telecommunications Conference*, Taipei, Taiwan, Nov. 2002, pp. 201–206.

[37] Betz, J. W.
Effect of narrowband interference on GPS code tracking accuracy.
In *Proceedings of ION 2000 National Technical Meeting*, Anaheim, CA, Jan. 2000.

[38] Borio, D., O'Driscoll, C., and Lachapelle, G.
Coherent, noncoherent, and differentially coherent combining techniques for acquisition of new composite GNSS signals.
IEEE Transactions on Aerospace and Electronic Systems, **45**, 3 (July 2009), 1227–1240.

[39] Corazza, G. E. and Pedone, R.
Generalized and average likelihood ratio testing for post detection integration.
IEEE Transactions on Communications, **55**, 11 (Nov. 2007), 2159–2171.

[40] Jung, J.
Implementation of correlation power peak ratio based signal detection method.
In *Proceedings of the 2004 ION GNSS Conference*, Long Beach, CA, Sept. 2004, pp. 486–490.

[41] Gil-Pelaez, J.
Note on the inversion theorem.
Biometrika, **38**, 3-4 (Dec. 1951), 481–482.

[42] Lehner, A., SteingaB, A., and Schubert, F.
A location and movement dependent GNSS multipath error model for pedestrian application.
In *Proceedings of the 13th European Navigation Conference (NAVITEC)*, Naples, Italy, 2009.

[43] Broumandan, A., Nielsen, J., and Lachapelle, G.
Indoor GNSS signal acquisition performance using a synthetic antenna array.
IEEE Transactions on Aerospace and Electronic Systems, **47**, 2 (Apr. 2011), 1337–1350.

[44] Gupta, R. D. and Kundu, D.
Generalized exponential distribution: Existing results and some recent developments.
Journal of Statistical Planning and Inference, **137**, 11 (Nov. 2007), 3537–3547.

[45] Fantino, M. et al.
Signal compression for an efficient and simplified GNSS signal parallel acquisition.
In *Proceedings of the 21st International Technical Meeting of the Satellite Division of The Institute of Navigation (ION GNSS)*, Savannah, GA, Sept. 2008.

[46] Gupta, R. D. and Kundu, D.
Closeness of gamma and generalized exponential distribution.
Communication in Statistics - Theory and Methods, **32**, 4 (2003), 705–722.

[47] Geiger, B. C., Soudan, M., and Vogel, C.
On the detection probability of parallel code phase search algorithms in GPS receivers.
In *Proceedings of IEEE International Symposium on Personal, Indoor and Mobile Radio Communications*, Istanbul, Turkey, Sept. 2010, pp. 865–870.

[48] Win, M. Z., Pinto, P. C., and Shepp, L. A.
A mathematical theory of network interference and its applications.
Proceedings of the IEEE, **97**, 2 (Feb. 2009), 205–230.

[49] Pinto, P. C. and Win, M. Z.
Communication in a Poisson field of interferers - Part I: Interference distribution and error probability.
IEEE Transactions on Wireless Communications, **9**, 1 (July 2010), 2176–2186.

[50] Rabbachin, A. et al.
Cognitive network interference.
IEEE Journal on Selected Areas in Communications, **29**, 2 (Feb. 2011), 480–493.

[51] Win, M. Z.
A mathematical model for network interference.
In *IEEE Communication Theory Workshop*, Sedona, AZ, May 2007.

[52] Kingsman, J.
Poisson Processes. New York: Oxford University Press, 1993.

[53] Samorodnitsky, G. and Taqqu, M. S.
Stable Non-Gaussian Random Processes. London: Chapmann and Hall, 1994.

[54] Rabbachin, A. et al.
Non-coherent UWB communication in the presence of multiple narrowband interferers.
IEEE Transactions on Wireless Communications, **9**, 11 (Nov. 2010), 3365–3379.

Matthias Wildemeersch (S'09) received the MSc degree in electromechanical engineering from the University of Ghent, Belgium and the PhD degree in electrical engineering at the University of Twente, the Netherlands, in 2003 and 2013, respectively.

From 2008 to 2011 he was at the Joint Research Centre of the European Commission, where he worked on the impact assessment of interference related to GNSS. From 2012 to 2013, he was a research scientist at the Institute for Infocomm Research, Singapore, and since 2014 he is a postdoctoral research fellow at the Singapore University of Technology and Design (SUTD), where his work broadly covers the analysis of heterogeneous networks. His research interests span various aspects of wireless communications and signal processing and focus on the application of probability theory and stochastic geometry to green communications, cognitive radio, and interference mitigation.

He received the IEEE SPAWC 2013 Best Student Paper Award and is an awardee of the A*STAR Research Attachment Programme (2012-2013).

Cornelis H. Slump (M'85) received the M.Sc. degree in electrical engineering from Delft University of Technology, the Netherlands in 1979. In 1984 he obtained his Ph.D. in physics from the University of Groningen, the Netherlands.

From 1983 to 1989 he was employed at Philips Medical Systems in Best as head of a predevelopment group on image quality and cardiovascular image processing. In 1989 he joined the Network Theory group from the University of Twente, Enschede, the Netherlands. His main research interest is in detection and estimation, interference reduction and pattern analysis as a part of digital signal processing. In June 1999 he was appointed as a full professor and heads the Signals and Systems group.

Alberto Rabbachin (S'03-M'07) received the Master Degree in telecommunications engineering from the University of Bologna, Italy and the Ph.D. degree in electrical engineering from the University of Oulu, Finland, in 2001 and 2008, respectively.

In 2011 he joined the Laboratory for Information and Decision Systems (LIDS) at the Massachusetts Institute of Technology (MIT), where he is currently a Marie Curie Fellow. He was a postdoctoral researcher with the Institute for the Protection and Security of the Citizen of the European Commission Joint Research Center from 2008 to 2011. His research interests involve communication theory and stochastic geometry applied to real-problems in wireless networks including network secrecy, cognitive radio, ultrawide-band transceiver design, network synchronization, ranging techniques, and interference exploitation.

Dr. Rabbachin is an Editor of the *IEEE Communications Letters* and served as symposium and workshop chair in various IEEE conferences. He received the IEEE Communications Society William R. Bennett Prize in the Field of Communications Networking (2012), the IEEE Globecom best paper award (2010), the European Commission JRC best young scientist award (2010), and the Nokia Fellowship (2005, 2006). He is a recipient of the International Outgoing Marie Curie Fellowship (2011-2014).